

Optics Letters

Influenza virus immunosensor with an electro-active optical waveguide under potential modulation

JAFAR H. GHITHAN,¹ MONICA MORENO,² GUILHERME SOMBRIO,^{1,3} RAJAT CHAUHAN,²
MARTIN G. O'TOOLE,² AND SERGIO B. MENDES^{1,*}

¹Department of Physics and Astronomy, University of Louisville, Natural Science Building, Louisville, Kentucky 40208, USA

²Department of Bioengineering, University of Louisville, Lutz Hall, Louisville, Kentucky 40208, USA

³Instituto de Física, Universidade Federal do Rio Grande do Sul, Porto Alegre 91509, Brazil

*Corresponding author: sbmend01@louisville.edu

Received 25 January 2017; revised 28 February 2017; accepted 28 February 2017; posted 1 March 2017 (Doc. ID 285642);
published 17 March 2017

Here we report the development of a novel immunosensor-based strategy for label-free detection of viral pathogens by incorporating a sandwich bioassay onto a single-mode, electro-active, integrated optical waveguide (EA-IOW). Our strategy begins with the functionalization of the electro-active waveguide surface with a capture antibody aimed at a specific virus antigen. Once the target antigen is bound to the photonic interface, it promotes the binding of a secondary antibody that has been labeled with a methylene blue (MB) dye. The MB is a redox-active probe whose optical absorption can be electrically modulated and interrogated with high sensitivity by a propagating waveguide mode. In this effort, we have targeted the hemagglutinin (HA) protein from the H5N1 avian influenza A virus to demonstrate the capabilities of the EA-IOW device for detection and quantification of an important antigen. Our initial results for the HA H5N1 influenza virus show a remarkable limit of detection in the pico-molar range. © 2017 Optical Society of America

OCIS codes: (050.1950) Diffraction gratings; (310.2785) Guided wave applications; (300.6360) Spectroscopy, laser; (130.3120) Integrated optics devices; (130.6010) Sensors.

<https://doi.org/10.1364/OL.42.001205>

Influenza is one of the main causes of serious respiratory infection diseases, and it can be produced by several strains of different subtypes of the influenza virus [1]. Rapid detection and classification of influenza infection in its early stages is important for effective treatment with anti-viral medication and for recognition of potential pandemic events. Immunoassay-based influenza virus detection incorporating antibody-antigen interactions provides a promising means of detection due to their extraordinary specificity and binding affinity.

An important method currently deployed for influenza virus detection is the enzyme-linked immunosorbent assay

(ELISA) [2]. This method relies on the chemical activity of surface-adsorbed enzymes for production of chromophore species to be detected in the bulk environment, but such a process has a slow throughput and leads to time-consuming protocols. Recently, different transduction methodologies have been combined with immunoassays protocols for direct assessment of the surface-adsorbed probe species. A key technique has been fluorescence immunosensors [3] to identify either the whole influenza virus or an antigen produced by the influenza virus. However, a critical limitation in light emission transduction methodologies has been the presence of undesired background noise in the detected analytical signal. Surface plasmon resonance (SPR) with the device interface functionalized with an immunoassay has been another important transduction strategy; however, there have been challenges for point-of-care applications of SPR due to tight requirements for temperature and mechanical stability, unwanted interference from non-specific adsorption, and poor sensitivity to analytes of low molecular weight [4]. Since electrochemical analysis is an interfacial process that allows detection of analytes in small volumes and at reasonable costs, there has been extensive interest in developing electrochemical immunosensors [5,6]. However, due to background current originating from ions' motion in the electrolyte solution and formation of an electric double layer on the electrode interface (the non-faradaic current), the current signal from probe species undergoing electrochemical reactions on the device surface (i.e., the faradaic current from redox species) is invariably very small and difficult to detect by traditional electrochemical techniques using purely electrical measurements. An alternative has been spectroelectrochemical methods in which a probing light wavelength is spectrally tuned to interrogate an optical transition associated with the electrochemically driven electron-transfer process of the surface-adsorbed redox molecules and is optically blind to the ions present in the electric double layer structure. Such an approach provides a superior route to investigate redox processes in molecular adsorbates by avoiding non-faradaic

components that typically hinder conventional electrochemical approaches using electrical signals alone. To enhance the interaction of a probing light beam and the surface-adsorbed redox species, a novel optical impedance spectroscopy technique based on a single-mode, electro-active, integrated optical waveguide (EA-IOW) was developed by us to investigate electrochemical properties of redox adsorbates with extremely high sensitivity [7].

Based on this groundwork [7], we describe here a novel immunosensor-based strategy for direct detection of important viral pathogens by incorporating a sandwich bioassay on a single-mode, EA-IOW platform. In this effort, we have targeted the hemagglutinin (HA) protein from the H5N1 avian influenza A virus to demonstrate the capabilities of the EA-IOW device for detection and quantification of a critical influenza antigen. Our immunoassay consisted of a monoclonal anti-H5 (H5N1) antibody bound to the EA-IOW device to create an interface that is prepared to recognize and capture the target HA protein. Once these HA antigens are captured on the device surface, they promote the immobilization of a polyclonal secondary antibody that has been labeled with methylene blue (MB) dye. Because the MB dye features a substantial and reversible change in optical absorption throughout a transition in the oxidation state (see inset in Fig. 1), it presents a unique optical probe that can be electrically controlled.

The overall experimental setup for this work is schematically represented in Fig. 2. At the heart of this configuration (see Fig. 1) is a multilayer (alumina/silica/indium tin oxide), single-mode EA-IOW with a pair of diffraction grating couplers; fabrication details of this optically transparent and conductive photonic device have been described by us elsewhere [7,8]. Here, an electrochemical flowcell with a three-electrode configuration (working, reference, and counter electrodes) was deployed to provide an electrochemically controlled aqueous environment in the superstrate region of the photonic device. The electrochemical flowcell included optical ports to couple a laser beam in and out of the EA-IOW device. A linearly transverse-electric polarized laser beam (with a wavelength of 610 nm or 633 nm) was aimed towards the edge of the input grating coupler, and an angular alignment through a rotation stage was performed to maximize the coupled power into the single-mode EA-IOW platform. After propagating for about 3.4 cm along the waveguide, the guided beam was outcoupled to free space by the second integrated diffraction grating. An

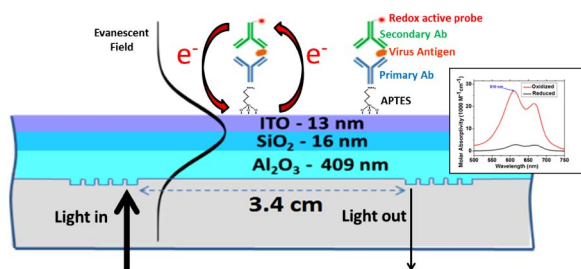


Fig. 1. Structure of the multilayer, single-mode EA-IOW device functionalized with a sandwich bioassay: an APTES monolayer, covalently bounded primary (capture) antibody, virus protein (antigen), and secondary antibody conjugated with the methylene blue redox-active optical probe. Inset: spectral molar absorptivity of methylene blue after conjugation with the secondary antibody at different oxidation states.

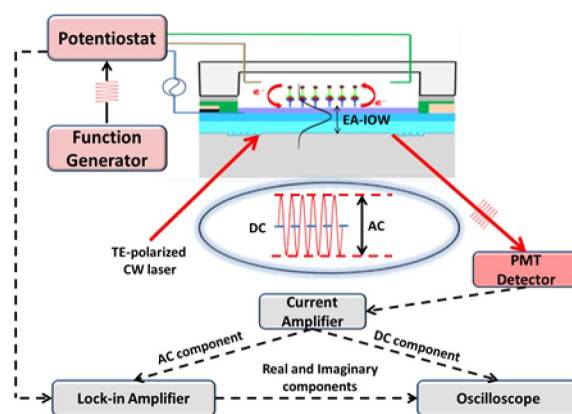


Fig. 2. Experimental setup includes a potentiostat for electrical control of the EA-IOW interface, laser light source, photo-multiplier detector, current amplifier, lock-in amplifier, and an oscilloscope for data collection.

optical fiber was deployed to collect the outcoupled optical signal and transfer it to a photomultiplier detector (PMT, H5783, Hamamatsu), which was connected to a low-noise current pre-amplifier (SR570, Stanford Research Systems). The optical signal was monitored while a potentiostat (CHI 660D, CH Instruments, Inc.) was used to control the electric potential applied to the working electrode (indium tin oxide [ITO] film) on the surface of the EA-IOW device; applied potential was referenced against an Ag/AgCl electrode in 1 M KCl solution. For AC-modulated measurements, the detected optical signal from the current pre-amplifier was sent to a lock-in amplifier (SR830 DSP, Stanford Research Systems), and the applied potential signal from the potentiostat was used for synchronization. A function generator (DS345, Stanford Research Systems) connected to the potentiostat provided a continuous sinusoidal wave to electrically drive the EA-IOW working electrode. An oscilloscope (DSO8104A Infiniium, Agilent) was deployed to read and record all signal traces.

To create an interface that promotes adsorption and conjugation of successive protein monolayers, the ITO surface of the EA-IOW platform was first functionalized with a (3-Aminopropyl) triethoxysilane (APTES) monolayer [9]. Next, the EA-IOW device was mounted into the electrochemical flowcell and the ITO/APTES interface was *in situ* functionalized with capture (primary) antibody species by injecting a solution of monoclonal antibody-H5 (H5N1) at a concentration of 2 $\mu\text{g}/\text{mL}$. After incubation of the EA-IOW device with the capture antibody solution for approximately 1 h, the flow-cell was thoroughly rinsed with a phosphate buffered saline (PBS) solution to remove unbound species. Next, a solution containing HA protein of the H5N1 influenza virus was injected into the flowcell and allowed to bind to the surface-bound capture antibodies before rinsing again with PBS. Finally, a MB-labeled polyclonal secondary antibody (MB-Ab) solution (concentration = 10 $\mu\text{g}/\text{mL}$) was injected to target the virus protein species residing on the EA-IOW surface before the cell was rinsed again. The presence of the surface-bound MB-Ab species was then optically interrogated while an electric potential was applied to the photonic device to control the oxidation state and, therefore, the optical absorption of the

probe. In this work, we have used virus protein solutions with the following concentrations: 200, 100, 20, and 0 ng/mL. After data collection at each specific concentration of the virus protein solution, we were able to reverse the interaction between the capture antibody and the ITO/APTES surface by sonicating the EA-IOW device in a potassium carbonate solution (pH 9–11) and easily renew the sensing interface for the next set of measurements.

First, optical absorbance data were collected with the EA-IOW platform under cyclic voltammetry (CV) potential modulation (see Supplemental Information in [7] for calculation details). The data for a virus protein solution at a concentration of 200 ng/mL are described by the red trace in Fig. 3. As the applied potential in the CV scans crosses the formal potential of the MB-Ab molecule (at about -0.2 V), it triggers an associated optical absorbance change that is clearly detected. In addition, the measured absorbance, A , allows the determination of the total surface density of the adsorbed probe species [10] by $\Gamma = A/(S\epsilon)$, where S is the sensitivity factor of the EA-IOW device and ϵ is the molar absorptivity of the redox probe; such calculation gave us a value of $\Gamma = 388$ fmol/cm². The black trace in Fig. 3 corresponds to data collected when the virus antigen was absent from the solution. The negligible absorbance signal (and redox transition) in this data reports negligible amounts of MB-Ab on the EA-IOW surface when the virus protein is absent and confirms that non-specific adsorption of the probe has been kept to a minimum at the functionalized interface. Those two experimental results confirm the ability of the EA-IOW platform to monitor the presence of the HA virus protein through the optical signal of the biologically matched redox probe.

Although CV modulation provides a clear and straightforward identification of the redox process, an improved signal-to-noise ratio with faster acquisition times can be obtained by applying an AC potential modulation on the EA-IOW platform in combination with synchronous detection from a lock-in amplifier. Figure 4(a) shows the amplitude of the modulated absorbance signal (see calculation details in [7]) versus the

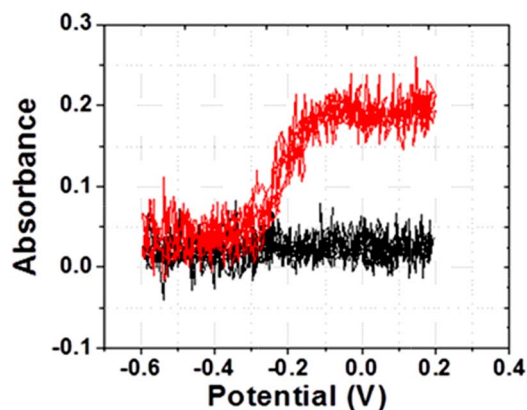


Fig. 3. Optical absorbance at 610 nm as measured by the EA-IOW platform under CV scans (scan rate = 20 mV/s). Red trace corresponds to data collected when the EA-IOW device functionalized with APTES and primary Ab was exposed to HA virus antigen (200 ng/mL) and MB-labeled secondary Ab (10 µg/mL). Black trace corresponds to data when the EA-IOW device functionalized under the same protocol was exposed to just MB-labeled secondary Ab (10 µg/mL), and in this instance the virus antigen was absent from the solution.

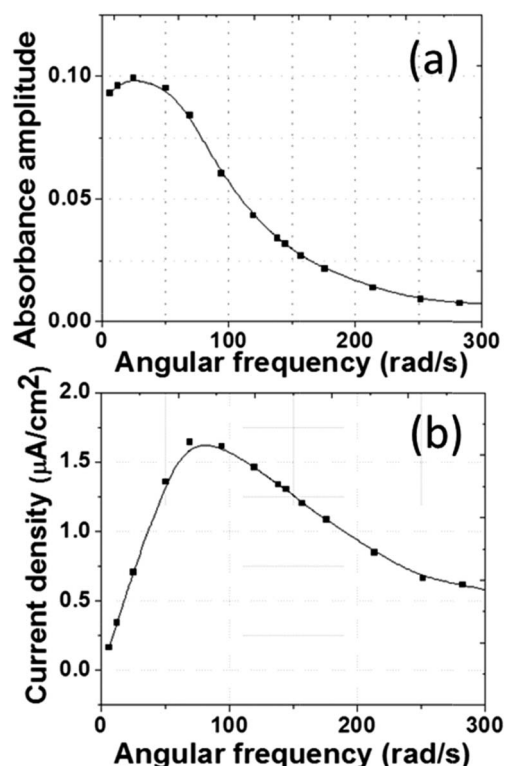


Fig. 4. (a) Absorbance amplitude measured with the functionalized EA-IOW device under AC potential modulation. Potential modulation amplitude = 30 mV, DC bias potential = -220 mV, laser wavelength = 633 nm, and virus protein concentration = 200 ng/mL. (b) Faradaic current density, as determined from the optical absorbance data in (a), showing a resonance frequency (at about 50 rad/s) associated with the electron transfer kinetic of the MB-Ab redox probe on the functionalized EA-IOW interface.

angular frequency of an AC potential modulation applied to the EA-IOW device that has been fully functionalized with the immunoassay to detect the virus antigen through the redox probe (MB-Ab). The collected optical data then allow the determination of the corresponding faradaic current density [7], which is shown in Fig. 4(b). As observed, the faradaic current density features a peak value centered at about 50 rad/s, which is associated with the electron transfer rate of the redox event under the interfacial conditions present on the electrode surface of the photonic device.

Once the optimum angular frequency has been determined (50 rad/s), an AC voltammetric technique at different DC bias potentials was applied while optical data were collected with the EA-IOW platform. A potential modulation with an amplitude of 30 mV was used, and the DC bias potential was varied over a range (-360 mV to $+40$ mV) encompassing the formal potential of the redox process of our probe. Different concentrations of the virus protein solution were tested. As shown in Fig. 5(a), a plot of the faradaic current density against the DC bias potential displays a maximum intensity at approximately -170 mV. As the DC bias potential is detuned from the formal potential (away from -170 mV) of our probe, the analytical signal decreases towards zero. The peak intensity of the faradaic current density reported by the redox probe is proportional to the surface concentration of the target antigen and provides a

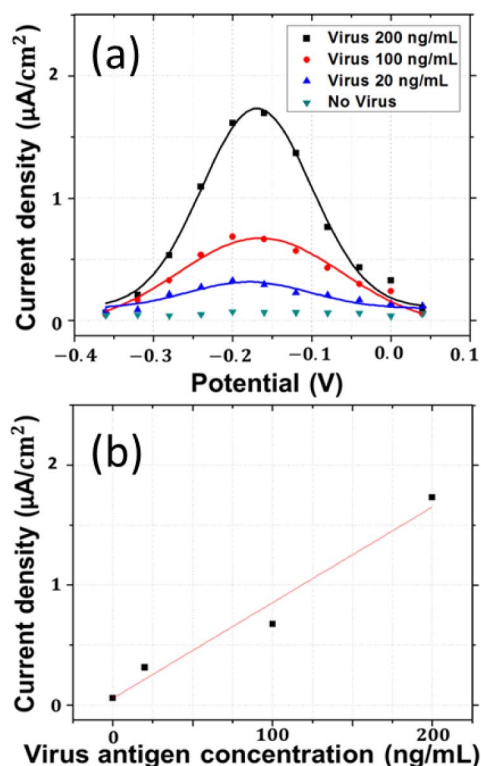


Fig. 5. (a) Faraday current density from the redox probe (MB-labeled secondary Ab) for different volume concentrations of the virus antigen. Measurements obtained under AC potential modulation where the faradaic current density is measured under different bias potential. (b) Maximum of the faradaic current density for each volumetric concentration of the virus antigen, which allows us to determine the limit of detection. Laser wavelength = 610 nm, angular frequency = 50 rad/s, amplitude modulation = 30 mV.

direct route to the quantification of the virus analyte. From the AC voltammetric data, the limit of detection was then determined by plotting the corresponding peak intensity of the current density for the different bulk concentrations of the virus antigen solution, as shown in Fig. 5(b). From the experimental data, a standard 3-sigma limit of detection was determined to

be about 4 ng/mL or 77 pico-molar (pM) for the virus antigen under test in our platform. Such a performance figure already surpasses several technologies currently deployed in clinics and places this novel strategy at the frontiers of the state of the art [11].

In summary, we have successfully combined the high sensitivity of a single-mode EA-IOW platform with a biologically specific sandwich immunoassay to demonstrate a novel strategy for pathogen analysis. Our analytical signal is linked uniquely to both the spectral and electrochemical properties of a redox probe designed to specifically recognize a target antigen. Those selective features are expected to minimize unwanted signals from interferents present in clinical samples. An AC voltammetric technique scanned across the formal potential of the redox probe provides a self-referenced detection protocol for direct quantification of the virus analyte in relatively small times. Our preliminary experimental results for the influenza A (H5N1) HA protein have reached an outstanding level of detection, even though several features can still be optimized in our technology to further improve device performance.

Funding. Jewish Heritage Fund for Excellence.

REFERENCES

1. K. Yohannes, P. Roche, J. Spencer, and A. Hampson, *Commun. Dis. Intell.* **27**, 162 (2003).
2. F. He, R. D. Soejodono, S. Murtini, M. Goutama, and J. Kwang, *BMC Microbiol.* **10**, 330 (2010).
3. Y. Li, M. Hong, B. Qiu, Z. Lin, Y. Chen, Z. Cai, and G. Chen, *Biosens. Bioelectron.* **54**, 358 (2014).
4. X. Zhang, H. Ju, and J. Wang, *Electrochemical Sensors, Biosensors and their Biomedical Applications* (Elsevier, 2008), p. 247.
5. A. Sirko, W. Zagorski-Ostojka, H. Radecka, J. Radecki, U. Jarocka, and R. Sawicka, *Biosens. Bioelectron.* **55**, 301 (2014).
6. Y. M. Zhou, Y. Z. Wu, G. L. Shen, and R. Q. Yu, *Sens. Actuators B* **89**, 292 (2003).
7. X. Han and S. B. Mendes, *Anal. Chem.* **86**, 1468 (2014).
8. X. Han and S. B. Mendes, *Thin Solid Films* **603**, 230 (2016).
9. M. A. Aziz, S. Patra, and H. Yang, *Chem. Commun.* **14**, 4607 (2008).
10. S. B. Mendes and S. S. Saavedra, *Appl. Opt.* **39**, 612 (2000).
11. Comparison of Biomolecular Interaction Techniques—Xantec Bioanalytics GmbH, 2016, http://www.xantec.com/technotes/comparison_of_biomolecular_interaction_techniques.php.